

Fractal Analysis of the UltraVISTA Galaxy Survey

Sharon Teles,^{1*} Amanda R. Lopes,^{2†} and Marcelo B. Ribeiro^{1,3‡§}

¹Valongo Observatory, Universidade Federal do Rio de Janeiro, Brazil

²Department of Astronomy, Observatório Nacional, Rio de Janeiro, Brazil

³Physics Institute, Universidade Federal do Rio de Janeiro, Brazil

15 December 2020

ABSTRACT

This paper seeks to test if the large-scale galaxy distribution can be characterized as a fractal system. Tools appropriate for describing galaxy fractal structures with a single fractal dimension D in relativistic settings are developed and applied to the UltraVISTA galaxy survey. A graph of volume-limited samples corresponding to the redshift limits in each redshift bins for absolute magnitude is presented. Fractal analysis using the standard Λ CDM cosmological model is applied to a reduced subsample in the range $0.1 \leq z \leq 4$, and the entire sample within $0.1 \leq z \leq 6$. Three relativistic distances are used, the luminosity distance d_L , redshift distance d_z and galaxy area distance d_G , because for data at $z \gtrsim 0.3$ relativistic effects are such that for the same z these distance definitions yield different values. The results show two consecutive and distinct redshift ranges in both the reduced and complete samples where the data behave as a single fractal galaxy structure. For the reduced subsample we found that the fractal dimension is $D = (1.58 \pm 0.20)$ for $z < 1$, and $D = (0.59 \pm 0.28)$ for $1 \leq z \leq 4$. The complete sample yielded $D = (1.63 \pm 0.20)$ for $z < 1$ and $D = (0.52 \pm 0.29)$ for $1 \leq z \leq 6$. These results are consistent with those found by [Conde-Saavedra et al. \(2015\)](#), where a similar analysis was applied to a much more limited survey at equivalent redshift depths, and suggest that either there are yet unclear observational biases causing such decrease in the fractal dimension, or the galaxy clustering was possibly more sparse and the universe void dominated in a not too distant past.

Key words: cosmology – fractals – galaxy distribution – UltraVISTA survey

1 INTRODUCTION

The *fractal galaxy distribution hypothesis* is an approach for the description of the large-scale structure of the Universe which assumes that this distribution is formed by a fractal system. This approach characterizes the system by means of its key feature, the *fractal dimension* D , which is basically a way of quantifying the irregularity of the distribution ([Mandelbrot 1983](#)). In the context of the large-scale structure of the Universe, D essentially measures galactic clustering sparsity or, complementary, the dominance of voids. Values of D smaller than 3, the topological dimension where the fractal structure is embedded, means irregular patterns in the structure. The smaller the values of D , the more sparse, or void dominated, is the galactic clustering.

The determination of the possible fractal properties of a given galaxy distribution with data gathered from a galactic survey is the subject of *fractal analysis*, where standard techniques of fractal geometry are applied to a given galaxy distribution dataset in or-

der to calculate the fractal dimension ([Pietronero 1987](#)). There are two ways in which this analysis can be performed: the single fractal approach or the multifractal one ([Coleman & Pietronero 1992](#); [Ribeiro & Miguelote 1998](#)).

Describing a fractal system by means of a *single fractal dimension* is the simplest approach, since it basically reduces the quantification of the irregular patterns within the system by means of a unique value for D . The single fractal approach is also capable of describing more complex distributions, since a system can exhibit different values of D at different distance ranges, that is, different scaling ranges may possess different single values for D . This situation means a succession of single fractal systems at different data ranges ([Sylos Labini et al. 1998](#)).

Differently from the single fractal approach, the *multifractal* one characterizes the fractal system by several fractal dimensions in the same scaling range, that is, a whole spectrum of dimensions whose maximum value corresponds to the single fractal dimension the structure would have if it were treated as a single fractal. The multifractal approach is applied when quantities like galactic luminosity or mass have a distribution, that is, they range between very different values. Hence, this is a generalization of D that includes such distributions and the maximum value of the multifractal spectrum corresponds to the single fractal dimension the system would

* E-mail: steles.ts@gmail.com

† E-mail: amandalopes1920@gmail.com

‡ E-mail: mbr@if.ufrj.br

§ Corresponding author

have if the studied quantity did not range, that is, as if it did not exhibit a multifractal pattern (Gabrielli et al. 2005).

The fractal analysis of galaxy surveys whose redshift measurements are bigger than $z \approx 0.1 - 0.3$ cannot be done without considering relativistic effects. This is because D is determined from plots of volume density vs. distance, which means volume-limited samples, and when one determines galaxy distances at those ranges relativistic effects become strong enough so that one is faced not with one distance value, but several different ones whose difference increases as z increases. That happens because relativistic cosmological models do not possess a single distance definition (Ellis 1971, 2007; Holanda et al. 2010) and, therefore, different distance values can be assigned for a galaxy with an empirically determined value of z , and the range where those differences become significant also depends on the chosen cosmological model. As a result, relativistic effects cannot be neglected when performing fractal analysis of galaxy distributions whose redshift data are gathered beyond those redshift ranges (Rangel Lemos & Ribeiro 2008).

In addition, as a consequence of relativistic effects even spatially homogeneous cosmological models like the standard Friedmann-Lemaître-Robertson-Walker (FLRW) will present observational inhomogeneities because observations are performed along the past light cone and at high redshift ranges distance measures required in the determination of volume densities will necessarily depart the local spatially homogeneous hypersurfaces of these models (Ribeiro 1992b, 1995, 2001b).

Fractal cosmology, that is, modelling the large-scale structure of the Universe by assuming that the galaxy distribution forms a fractal system, is an old subject previously known in the literature as *hierarchical cosmology*. Discussions regarding the possible hierarchical structuring of the Universe go as far back as the beginning of the 20th century (Charlier 1908, 1922; Einstein 1922; Seley 1922; Amoroso Costa 1929), and attempts to theoretically describe and empirically characterize this hierarchical galaxy structure followed suit in later decades (Carpenter 1938; De Vaucouleurs 1960, 1970; Wertz 1970, 1971; Haggerty & Wertz 1972). The appearance of fractal geometry in the 1980s showed that the hierarchical galaxy structure discussed in these earlier studies has essentially the same features of galaxy distribution models that considered this distribution as a fractal system (Mandelbrot 1983; Pietronero 1987). In fact, the basic theoretical framework of these early hierarchical models turns out to lead to the same expressions as the ones originated from a fractal galaxy distribution model (Ribeiro 1994; Ribeiro & Miguelote 1998).

Newtonian cosmology was used in earlier hierarchical cosmology models (Wertz 1970, 1971; Haggerty & Wertz 1972), as well as in more recent fractal cosmology ones (Abdalla et al. 1999; Abdalla & Chirenti 2004). Relativistic cosmological models, both spatially homogeneous and inhomogeneous, which considered a fractal system embedded in a 4-dimensional spacetime along the observer’s past light cone, producing then relativistic fractal cosmologies, were developed later (Ribeiro 1992a, 1993; Abdalla et al. 2001; Ribeiro 2001a,b, 2005). More recently, several authors discussed relativistic cosmological models with fractal features either theoretically (Mureika & Dyer 2004; Mureika 2007; Sylos Labini 2011; Nogueira 2013; Hossienkhani et al. 2018; Sadri et al. 2018; Cosmai et al. 2019; Jawad et al. 2019) or by attempting to apply fractal features to different observational scenarios using Newtonian or relativistic models (Jones et al. 1988; Martínez 1990; Pan & Coles 2000; Gaite 2007; Stahl 2016; Raj et al. 2019; Souza 2020).

Of particular interest to this paper is the study presented by

Conde-Saavedra et al. (2015, from now on CS2015), which stands on the middle ground between the two previously mentioned types of works in the sense that it developed both theoretical tools capable of characterizing a fractal system at high redshift by fully considering relativistic effects, and also performed data analysis of high redshift galaxy data in order to actually measure the single fractal dimension of the structure at different scale ranges having deep redshift values, that is, far from our present spatial foliation of spacetime as described in a 3+1 formalism of general relativity. This study concluded that for $z \lesssim 1.3 - 1.9$ the average single fractal dimension that considered all distance definitions used in the paper resulted in $D = 1.4^{+0.7}_{-0.6}$, whereas for redshift values higher than this approximate threshold they obtained $D = 0.5^{+1.2}_{-0.4}$.

This paper aims at applying the fractal analysis methodology used by CS2015 to a different galaxy sample, but with two major differences. First, the fractal analysis is applied to the UltraVISTA galaxy survey, which has measured redshift values of about 220k galaxies, a considerably larger galaxy sample than the FORS Deep Field dataset of 5.5k galaxies used in CS2015. Second, samples are obtained directly from measured redshift data instead of the indirect luminosity function methodology employed by CS2015. A graph of absolute magnitudes in terms of redshifts shows that the UltraVISTA galaxies scale with redshift bins, providing then a volume-limited subsample appropriate for a fractal analysis. Nevertheless the whole survey data was also subject to fractal analysis for comparison purposes.

As a consequence of these different approaches, the results obtained here are clearly improved once compared to the ones achieved by CS2015, namely, a better defined threshold for low and high scaling ranges, smaller uncertainties and results more in line with each other considering all cosmological distance definitions used in both studies. Our calculations showed that summing up all results and uncertainties obtained with the employed distance definitions we concluded that both the subsample and entire survey data of the UltraVISTA catalog can be well characterized as a fractal galaxy distribution system possessing two consecutive scaling ranges with the following single fractal dimensions. The subsample resulted in $D = (1.58 \pm 0.20)$ for $z < 1$, and $D = (0.59 \pm 0.28)$ for $1 \leq z \leq 4$, whereas the complete sample yielded $D = (1.63 \pm 0.20)$ for $0.1 < z < 1$, and $D = (0.52 \pm 0.29)$ for $1 \leq z \leq 6$.

The plan of the paper is as follows. Section 2 develops standard tools of fractal geometry necessary for modelling the large-scale galaxy distribution as a fractal system in both Newtonian and relativistic frameworks, comprising review material extensively discussed and developed elsewhere plus a few additional remarks. This is included here for a self-contained presentation. Section 3 describes the observational details of the UltraVISTA galaxy survey relevant to this work, and discusses the data handling required for the application of fractal tools to this specific dataset. Section 4 presents the results of the fractal analysis of the UltraVISTA galaxy distribution. Discussions and conclusions are the subject of Section 5.

2 FRACTAL COSMOLOGY

It has been known since Mandelbrot’s (1983) original studies that fractal systems are characterized by power-laws. In fact, the early hierarchic cosmological models were connected to fractals exactly because galaxy density distribution data showed power-law features (e.g., De Vaucouleurs 1970). Hence, the early definitions and concepts used in the hierarchical cosmologies are the appropriate

ones to start with. As it turns out these quantities form a set of very simple concepts and definitions able to characterize single-fractal-dimension galaxy distributions. Moreover, they are easily and straightforwardly adapted to a relativistic setting, albeit with some limitations.

2.1 Newtonian hierarchical (fractal) cosmology

Let V_{obs} be the *observational volume* defined by the expression below,

$$V_{\text{obs}} = \frac{4}{3}\pi(d_{\text{obs}})^3, \quad (1)$$

where d_{obs} is the *observational distance*. The *observed volume density* γ_{obs}^* is defined as follows,

$$\gamma_{\text{obs}}^* = \frac{N_{\text{obs}}}{V_{\text{obs}}}, \quad (2)$$

where N_{obs} is the *observed cumulative number counts* of cosmological sources, that is, galaxies. Clearly γ_{obs}^* gives the number of sources per unit of observational volume out to a distance d_{obs} .

The *key hypothesis* underlining the hierarchical (fractal) galaxy distribution relates the cumulative number counts of observed cosmological sources and the observational distance by a phenomenological equation called the *number-distance relation* (Wertz 1970; Pietronero 1987), whose expression yields,

$$N_{\text{obs}} = B (d_{\text{obs}})^D, \quad (3)$$

where B is a positive constant and D is the fractal dimension. This expression forms the basic hypothesis of the *Pietronero-Wertz hierarchical (fractal) cosmology* (Ribeiro 1994; Ribeiro & Miguelote 1998, and references therein).

Note that since N_{obs} is a cumulative quantity, if beyond a certain distance there are no longer galaxies then N_{obs} no longer increases with d_{obs} . If instead objects are still detected and counted then it continues to increase. Observational biases may possibly affect its rate of growth, leading to an intermittent behavior, however, N_{obs} must grow or remain constant, and thus the exponent in Eq. (3) must be positive or zero.

One may also define a second density in this context, the *observed differential density* γ_{obs} . Its expression may be written as follows (Wertz 1970, 1971),

$$\gamma_{\text{obs}} = \frac{1}{4\pi(d_{\text{obs}})^2} \frac{dN}{d(d_{\text{obs}})}. \quad (4)$$

From this definition it is clear that γ_{obs} gives the rate of growth in number counts, or more exactly in their density, as one moves along the observational distance d_{obs} .

Substituting Eqs. (1) and (3) into Eqs. (2) and (4) we respectively reach at two forms of the *De Vaucouleurs density power-law* (Pietronero 1987; Ribeiro 1994),

$$\gamma_{\text{obs}}^* = \frac{3B}{4\pi} (d_{\text{obs}})^{D-3}, \quad (5)$$

$$\gamma_{\text{obs}} = \frac{DB}{4\pi} (d_{\text{obs}})^{D-3}. \quad (6)$$

Thus, if the observed galaxy distribution behaves as a fractal system with $D < 3$, that is, if it follows the number-distance relation (3), both observational densities above decay as power-laws. If $D = 3$ the distribution is said to be *observationally homogeneous*, as both densities become constant and distance independent. Note that the two power-laws above allow the empirical determination of different

single fractal dimensions in two or more scaling ranges dependent on the observational distance.

The ratio between the two forms of the De Vaucouleurs density power-law yields,

$$\frac{\gamma_{\text{obs}}}{\gamma_{\text{obs}}^*} = \frac{D}{3}. \quad (7)$$

For an observationally homogeneous galaxy distribution this ratio must be equal to one, whereas an irregular distribution forming a single fractal system will have $0 \leq (\gamma_{\text{obs}}/\gamma_{\text{obs}}^*) < 1$.

There are two important remarks to be made regarding the densities defined by Eqs. (2) and (4). First, both γ_{obs}^* and γ_{obs} are radial quantities and, therefore, should not be understood in statistical sense because they do not average all points against all points. Second, although both quantities are in principle equally applicable to cosmological objects, as pointed out by Conde-Saavedra et al. (2015, Secs. 4.2.1, 4.2.2) γ_{obs} is unsuitable for high redshift measures because the term $dN_{\text{obs}}/d(d_{\text{obs}})$ in Eq. (4) increases, reaches a maximum and then decreases, affecting the exponent at high values of z in such a way as producing spurious negative values for D at such ranges. As noted above, negative values for D are not possible due to the very definition of the number-distance relation (3) and, hence, γ_{obs} can only be safely used at relatively low redshift values, that is, $z \lesssim 1$ or at ranges smaller than the observed galaxy distribution histogram of galaxy numbers per redshift bins reaches its maximum.

So, for the reasons exposed above, from now on we shall only consider the volume density γ_{obs}^* in our calculations, since this density is not contaminated by spurious effects at $z > 1$.

2.2 Relativistic fractal cosmology

The expressions above can be applied as such in Newtonian cosmologies, but as far as relativistic cosmological models are concerned two important conceptual issues must be considered which alter the expressions above in specific ways.

First, in relativistic cosmology observations are located along the observer's past light cone. This means that even spatially homogeneous cosmologies like the FLRW will *not* produce observationally constant volume densities at high redshift values because it is theoretically impossible to expect that the observed volume density will become constant even at moderate redshift values in FLRW cosmologies (Conde-Saavedra et al. 2015, Sec. 2.1). The basic point here is that observational and spatial homogeneities are different concepts in relativistic cosmology, so it is theoretically possible to have a cosmological-principle-obeying spatially homogeneous cosmological model exhibiting observational inhomogeneity, as extensively discussed elsewhere (Ribeiro 1992b, 1994, 1995, 2001b, 2005; Rangel Lemos & Ribeiro 2008).

Second, both γ_{obs}^* and γ_{obs} are *average* densities defined in the fractal cosmology context, and, therefore, should *not* be confused with the local density appearing on the right hand side of Einstein equations. Moreover, densities in fractal cosmology are defined in terms of observational distances, which means that at high redshift d_{obs} will have different values for each distance definition at the same redshift value z . In other words, as distance in relativistic cosmology is a concept not uniquely defined (Ellis 1971, 2007; Holanda et al. 2010) we need to replace d_{obs} for d_i in the equations above, where the index will indicate the observed distance definition chosen to be calculated with specific redshift values. In this case the applicable distance definitions are the *redshift distance* d_z , *luminosity distance* d_L and *galaxy area distance* d_G , also known as *transverse comoving*

distance. The last two are connected by the Etherington reciprocity law (Etherington 1933; Ellis 2007) which reads as follows,

$$d_L = (1+z) d_G. \quad (8)$$

The redshift distance yields,

$$d_z = \frac{cz}{H_0}, \quad (9)$$

where c is the light speed and H_0 is the Hubble constant. This definition of d_z is, of course, only valid in the FLRW metric. Albani et al. (2007) and Iribarrem et al. (2012) showed that within the FLRW cosmology the densities defined by both d_L and d_z have empirical power-law properties, the same applying for d_G .

Another distance measure that can be defined in this context is the *angular diameter distance* d_A , also known simply as *area distance*, which is also connected to the quantities above by the reciprocity law, also known in the literature as the *cosmic distance duality relation* (Holanda et al. 2010, 2011, 2012; Zheng et al. 2020), which reads as follows,

$$d_L = (1+z)^2 d_A. \quad (10)$$

However, *densities* defined with d_A have the odd behavior of increasing as z increases, making this distance unsuitable to use in the context of a fractal analysis of the galaxy distribution (Ribeiro 2001b, 2005; Rangel Lemos & Ribeiro 2008).

Bearing these points in mind, the expressions above become applicable to relativistic cosmology models once they are rewritten as below,

$$d_{\text{obs}} = d_i, \quad (11)$$

$$V_{\text{obs}} = V_i = \frac{4}{3}\pi(d_i)^3, \quad (12)$$

$$N_{\text{obs}} = N_i = B_i (d_i)^{D_i}, \quad (13)$$

$$\gamma_{\text{obs}}^* = \gamma_i^* = \frac{N_i}{V_i} = \frac{3B_i}{4\pi} (d_i)^{D_i-3}, \quad (14)$$

where $i = (L, z, G)$ according to the distance definition used to calculate the volume density. The proportionally constant B_i of the number-distance relation will, therefore, be attached to each specific distance definition, this being also true for the fractal dimension D_i , because N_i is counted considering the limits of each distance definition. Hence, for a given z each d_i yields its respective V_i , N_i , B_i and D_i , which means that all quantities become attached to a certain distance definition.

As final points, first it is important to mention that although the fractal analysis discussed above can be performed using d_L in any cosmological model, the same is not true for d_z because its definition in Eq. (9) is restricted to FLRW cosmologies. Regarding d_G , it has been previously shown that calculating the volume density in the Einstein-de Sitter cosmology using d_G results in $\gamma_G^* = \text{constant}$ (Ribeiro 2001b, pp. 1718, 1723, 1724), which seemed to indicate d_G as an unsuitable distance definition to be used in fractal analysis. Nevertheless, later works showed that such behavior is cosmology dependent, not being valid in other FLRW models (Albani et al. 2007, fig. 7; Iribarrem et al. 2012, figs. 2-5; Conde-Saavedra et al. 2015, figs. 3-4). This finding justifies the inclusion of γ_G^* in the present study.

Second, the concepts above indicate that reasoning that regards

the fractal approach to the galaxy distribution only at low redshift ranges are not applicable to the analysis performed in this paper. As the light cone is a relativistic concept, confusion arises if one does not acknowledge the difference between spatial and observational volume densities. It is in the latter spacetime locus that astronomy is made and where fractality in the sense of this work may be detected. Hence, observed fractal features appear only by correctly manipulating the FLRW observational quantities along the observer's past light cone at ranges where the null cone effects become relevant as far as distance definitions are concerned (Ribeiro 1995, 2001b, 2005; Rangel Lemos & Ribeiro 2008). These effects form the very core of the present analysis.

3 FRACTAL ANALYSIS

As this study seeks to empirically ascertain whether or not the fractal galaxy distribution hypothesis holds at very large-scales of the observed Universe, we chose to perform a fractal analysis with the data provided by the UltraVISTA galaxy survey, since it contains hundreds of thousands of galaxies with measured redshifts. Let us present next some details about this survey and how the fractal analysis was performed in their data.

3.1 The UltraVISTA galaxy survey

Our data are based on the first data release of the UltraVISTA galaxy survey, which is centered on the COSMOS field (Scoville et al. 2007) with an effective area of 1.5 deg^2 . Observations were made in 4 near infrared filters, Y , J , H and K_S , described in McCracken et al. (2012). Photometric redshifts were calculated by Ilbert et al. (2013) applying the SED fitting technique to 29 bands, the ones from UltraVISTA and a complementary set of broad and narrow bands from other surveys encompassing the ultraviolet, optical, near infrared and mid infrared regimes. The initial dataset consisted in a K_S -band selected ($K_S < 24$) sample of about 220k galaxies in the redshift range of $0.1 \leq z \leq 6$. Although the sample was originally divided into quiescent and star forming galaxies, such grouping is unimportant for the purposes of this study and, hence, all galaxies of both types were included in the subsample selection and analysis performed here. Fig. 1 shows the UltraVISTA survey's galaxy numbers distribution in terms of redshift. Figs. 2 and 3 respectively show the galaxy numbers distribution in terms of right ascension and declination.

3.2 Data selection

The fractal analytical tools discussed above require the establishment of volume limited samples. However, galaxy surveys are limited by apparent magnitude, so some methodology is needed to ascertain that reduced subsamples follow increasing redshift bins in order to render the reduced galaxy data distributed over limited volume bins. One way of doing this is by plotting the galaxies' absolute magnitudes in terms of their respective measured redshifts and then selecting galaxies below a certain absolute magnitude threshold defined by the limiting apparent magnitude of the survey. This can be done by using the usual expression below,

$$M = m - 5 \log d_L(z) - 25, \quad (15)$$

where M is the absolute magnitude, m is the apparent magnitude and d_L is given in Mpc. Next one needs to choose the apparent magnitude threshold m and its passband, as well as verifying if

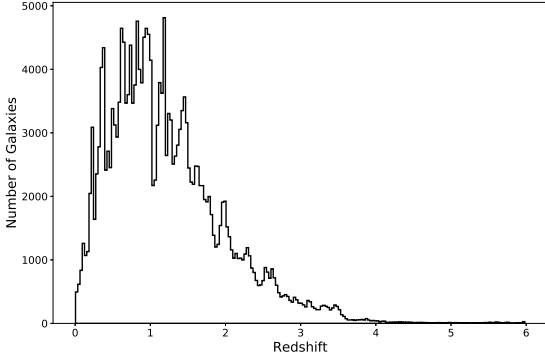


Figure 1. Histogram showing the galaxy distribution numbers in terms of redshift for the UltraVISTA survey dataset studied here. This graph has $\Delta z = 0.03$ as the redshift bins' size.

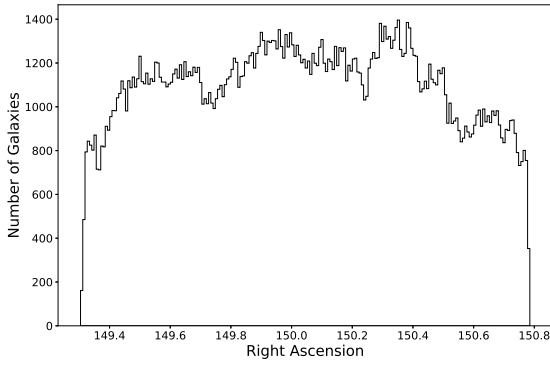


Figure 2. Histogram showing the galaxy distribution numbers in terms of right ascension (deg) for the UltraVISTA survey dataset studied here.

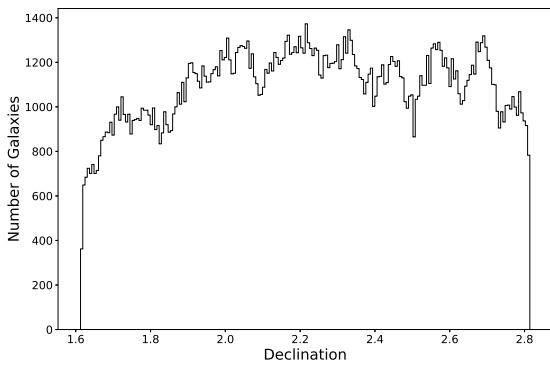


Figure 3. Histogram showing the galaxy distribution numbers in terms of declination (deg) for the UltraVISTA survey dataset studied here.

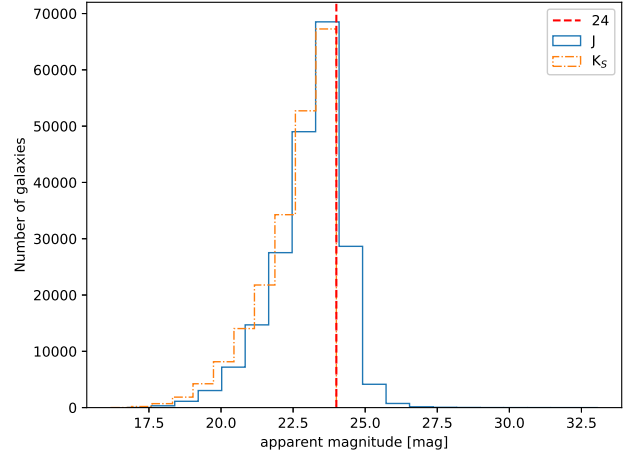


Figure 4. UltraVISTA galaxy numbers plotted in terms of apparent magnitudes in both the J and K_S passbands. The number distribution for both bandwidths peaks at apparent magnitudes equal to 24 indicated by the vertical line.

the resulting data is indeed, at least generally, distributed along the measured redshift bins, and then possibly establishing a redshift window for the final subsample distribution.

The UltraVISTA survey furnished absolute magnitudes calculated in the NUV , B , R and J passbands. The J -band is the best choice among those for our purposes here, since this near infrared filter is less affected by dust extinction. Fig. 4 shows an histogram of the UltraVISTA galaxy numbers in terms of apparent magnitudes in the K_S and J passbands. Clearly the number distribution peaks at the apparent magnitude value 24 for both wavebands, a fact that led us to choose $J = 24$ as our apparent magnitude threshold. Therefore, Eq. (15) can be rewritten according to the expression below, which provides the dividing line between the selected and unselected galaxies.

$$M_J = 24 - 5 \log d_L(z) - 25. \quad (16)$$

Fig. 5 shows a plot of the absolute magnitudes of 219300 UltraVISTA galaxies in the J -band against their respective measured redshifts. Green filled circles are those whose absolute magnitudes provided by the survey are smaller than M_J in Eq. (16), and are then inside the reduced subsample, whereas the open gray circles are outside this threshold. We noticed that the absolute magnitude cut based on the J -band corresponds to a volume-limited subsample because the data generally follow the redshift bins of increasing values. In addition, we also noticed that there are few galaxies at the tail of the distribution, so our subsample suffered a further cut at $z = 4$.

Hence, we end up with a *reduced UltraVISTA subsample* of 166566 galaxies cut by J -band absolute magnitudes M_J and limited up to $z = 4$. The remaining 52734 galaxies outside this subsample, that is, below the dividing line in Fig. 5 and having $z > 4$, were disregarded.

3.3 Data analysis

To obtain the observational distances d_i ($i = G, L, z$) from the calculated photometric redshift values one needs to choose a cosmological model. We assumed the FLRW cosmology with $\Omega_{m0} = 0.3$, $\Omega_{\Lambda 0} = 0.7$ and $H_0 = 70 \text{ km s}^{-1} \text{ Mpc}^{-1}$.

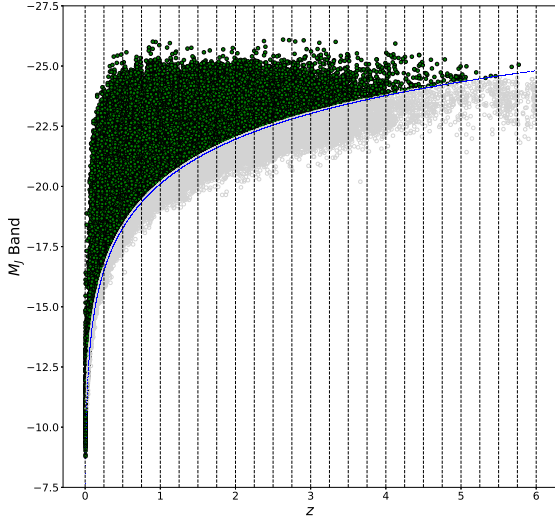


Figure 5. Absolute magnitudes in the J -band vs. redshift for all galaxies of the UltraVISTA survey. Green filled circles are galaxies having M_J smaller than the blue line cut given by Eq. (16), whereas open gray circles have bigger values for M_J .

The next steps were the establishment of the minimum redshift value z_0 from where to start the analysis, the respective minimum distances $d_{i_0} = d_{i_0}(z_0)$, and the incremental distance interval Δd_i . The data sorting process was initiated by counting the number of observed galaxies N_{i_1} in the first interval $d_{i_1} = d_{i_0} + \Delta d_i$ and calculating the respective volume density $\gamma_{i_1}^*$. This first interval defined the first bin. Then, the size of the bin was increased by Δd_i and values for N_{i_2} and $\gamma_{i_2}^*$ were obtained at the distance $d_{i_2} = d_{i_0} + 2\Delta d_i$. This algorithm was repeated n times until the last, and farthest, group of galaxies were included and all relevant quantities were also counted and calculated.

Different bin size increments Δd_i were tested for each distance definition in order to find out whether or not that would affect the results. This test turned out negative, which means that the obtained results are independent of bin size increment. We then chose $\Delta d_i = 200$ Mpc, value which was applied to all calculations and provided in the end a very reasonable amount of data points for each quantity from where simple linear regression analyses were able to be performed.

The final step was the determination of the fractal dimension itself. If the galaxy distribution really formed a fractal system, according to Eq. (14) the graphs of γ_i^* vs. d_i would behave as decaying power-law curves, and whose linear fit slopes in log-log plots allow for the fractal dimensions D_i of the distribution to be straightforwardly determined.

4 RESULTS

4.1 Reduced subsample

Graphs for log-log values of γ_i^* vs. d_i showed that to a good approximation the reduced UltraVISTA galaxy survey subsample sorted according to the criteria set at Sec. 3.2 conforms with what is predicted as if the galaxy distribution does form a fractal system. More-

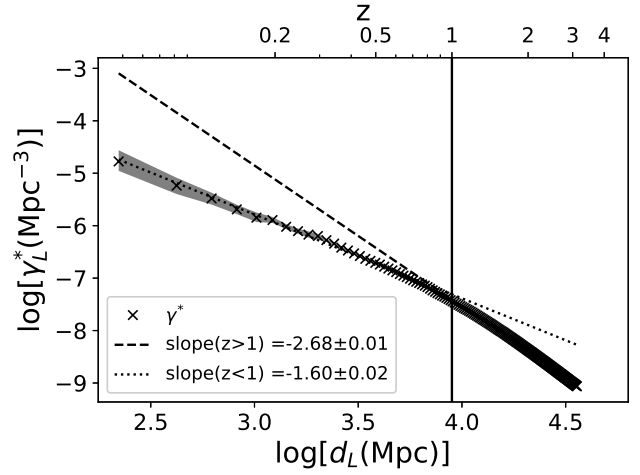


Figure 6. Graph showing the log-log results for γ_L^* vs. d_L obtained with the reduced UltraVISTA galaxy redshift survey dataset (see Sec. 3.2). The dotted line is the straight line fit for galaxies having $z < 1$, whereas the dashed line is for those with $z > 1$. The error area is in gray. According to Eq. (14) the fractal dimensions obtained from these data are $D_L = (1.40 \pm 0.02)$ for $z < 1$ and $D_L = (0.32 \pm 0.01)$ for $1 \leq z \leq 4$.

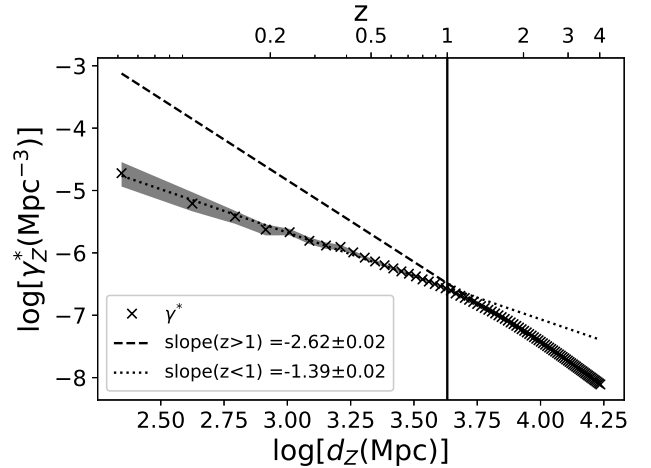


Figure 7. Graph showing the log-log results for γ_z^* vs. d_z obtained with the reduced UltraVISTA galaxy redshift survey dataset (see Sec. 3.2). The dotted line is the straight line fit for galaxies having $z < 1$, whereas the dashed line is for those with $z > 1$. The error area is in gray. According to Eq. (14) the fractal dimensions obtained from these data are $D_z = (1.61 \pm 0.02)$ for $z < 1$ and $D_z = (0.38 \pm 0.02)$ for $1 \leq z \leq 4$.

over, two power-law decaying regions were observed in the data, for $z < 1$ and $z > 1$, producing different single fractal dimensions.

Figs. 6 to 8 present the results for all distance definitions adopted here, from where it can be concluded that for $z < 1$ the fractal dimension is in the range 1.38 – 1.78, whereas for $1 \leq z \leq 4$ the resulting range is significantly smaller, 0.31 – 0.87. Table 1 collects all results.

In summary, the results above indicate that the UltraVISTA galaxy survey provided a galaxy distribution subsample dataset that can be described as a fractal system with the following two consecutive and approximate single fractal dimensions values: $D(z < 1) = (1.58 \pm 0.20)$ and $D(1 \leq z \leq 4) = (0.59 \pm 0.28)$. The

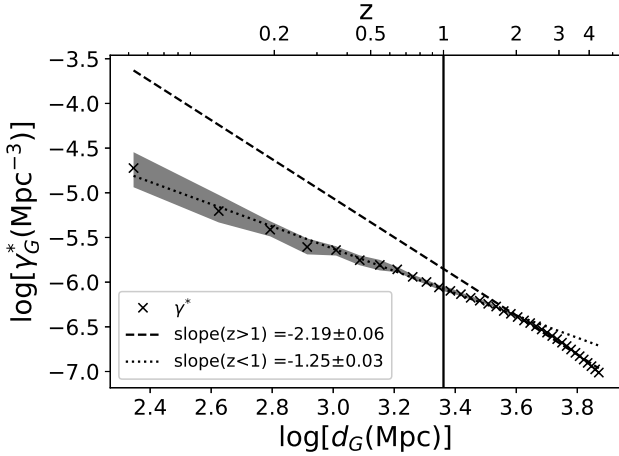


Figure 8. Graph showing the log-log results for γ_G^* vs. d_G obtained with the *reduced* UltraVISTA galaxy redshift survey dataset (see Sec. 3.2). The dotted line is the straight line fit for galaxies having $z < 1$, whereas the dashed line is for those with $z > 1$. The error area is in gray. According to Eq. (14) the fractal dimensions obtained from these data are $D_G = (1.75 \pm 0.03)$ for $z < 1$ and $D_G = (0.81 \pm 0.06)$ for $1 \leq z \leq 4$.

Table 1. Results in two redshift scales of the UltraVISTA galaxy survey fractal analysis in the *reduced* subsample (see Sec. 3.2). The single fractal dimensions D_L , D_z and D_G were obtained from this galaxy distribution respectively using the luminosity distance d_L , redshift distance d_z and galaxy area distance (transverse comoving distance) d_G .

	D_L	D_z	D_G
$z < 1$	1.40 ± 0.02	1.61 ± 0.02	1.75 ± 0.03
$1 \leq z \leq 4$	0.32 ± 0.01	0.38 ± 0.02	0.81 ± 0.06

possible reasons as why the fractal dimension is so much reduced at the deepest range $z > 1$ will be discussed below.

4.2 Complete (unselected) survey data

The fractal analysis of the UltraVISTA galaxy subsample, as defined in Sec. 3.2, were based in the plot of absolute magnitudes in the *J*-band in terms of the measured redshifts of the galaxies shown in Fig. 5. However, this plot also shows that even the galaxies outside the absolute magnitude cut are also distributed along increasing redshift bins, a fact that suggests that the whole sample may also be volume-limited. Hence, it is interesting to apply the same fractal methodology developed above not only to the subsample, but also to the whole survey data in order to compare the results.

Figs. 9-11 show the results of the fractal analysis of the complete UltraVISTA survey data. It is clear that the galaxy distribution also presents fractal features in two regions below and above the redshift value $z = 1$. The corresponding single fractal dimensions for each distance definitions adopted here were found to lie in the range $1.42 - 1.83$ for $z < 1$, whereas for $1 \leq z \leq 6$ the dimension is significantly smaller, in the range $0.23 - 0.81$. Table 2 collects these results and a comparison with the ones for the reduced subsample presented in Table 1 indicated results very much alike, although their respective uncertainties do not overlap.

So, it seems that the whole UltraVISTA galaxy survey can

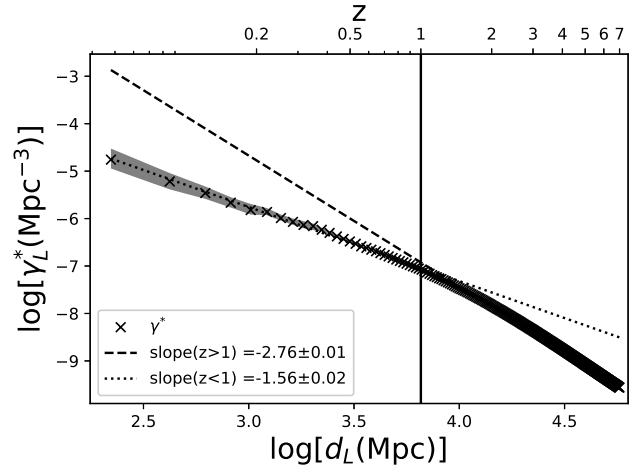


Figure 9. Graph showing the log-log results for γ_L^* vs. d_L obtained with the complete UltraVISTA galaxy survey dataset. The dotted line is the straight line fit for galaxies having $z < 1$, whereas the dashed line is for those with $z > 1$. The error area is in gray. According to Eq. (14) the fractal dimensions obtained from these data are $D_L = (1.44 \pm 0.02)$ for $z < 1$ and $D_L = (0.24 \pm 0.01)$ for $1 \leq z \leq 6$.

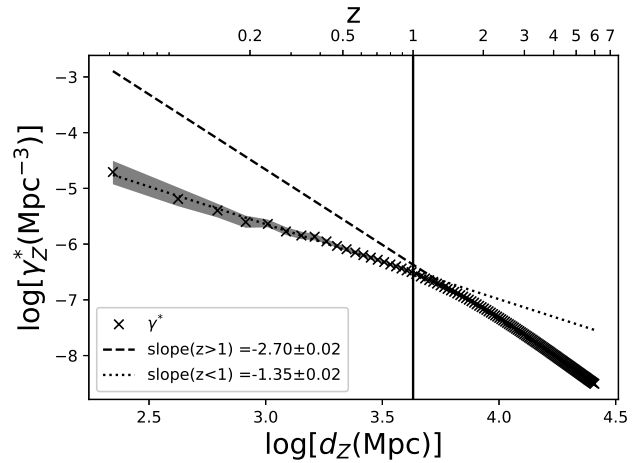


Figure 10. Graph showing the log-log results for γ_z^* vs. d_z obtained with the complete UltraVISTA galaxy survey dataset. The dotted line is the straight line fit for galaxies having $z < 1$, whereas the dashed line is for those with $z > 1$. The error area is in gray. According to Eq. (14) the fractal dimensions obtained from these data are $D_z = (1.65 \pm 0.02)$ for $z < 1$ and $D_z = (0.30 \pm 0.02)$ for $1 \leq z \leq 6$.

also be described as a fractal system having two consecutive single fractal dimensions: $D(z < 1) = (1.63 \pm 0.20)$ and $D(1 \leq z \leq 6) = (0.52 \pm 0.29)$.

5 CONCLUSIONS

This paper sought to empirically test if the large-scale galaxy distribution can be described as a fractal system. Tools originally developed for Newtonian hierarchical cosmology were extended and applied to relativistic cosmological models in order to possibly describe galaxy fractal structures by means of single fractal dimensions at deep redshift values. These tools were applied to the UL-

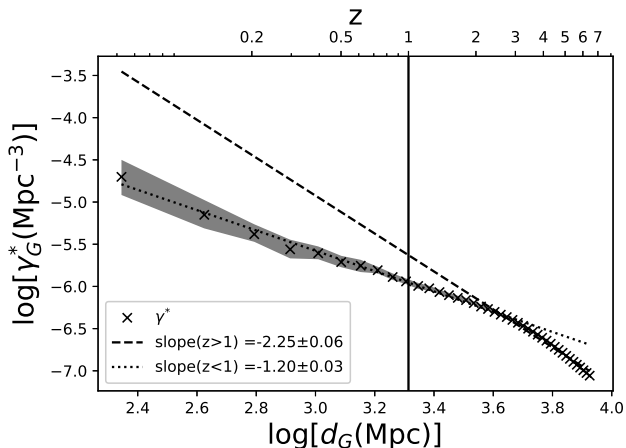


Figure 11. Graph showing the log-log results for γ_G^* vs. d_G obtained with the complete UltraVISTA galaxy survey dataset. The dotted line is the straight line fit for galaxies having $z < 1$, whereas the dashed line is for those with $z > 1$. The error area is in gray. According to Eq. (14) the fractal dimensions obtained from these data are $D_G = (1.80 \pm 0.03)$ for $z < 1$ and $D_G = (0.75 \pm 0.06)$ for $1 \leq z \leq 6$.

Table 2. Results in two redshift scales of the UltraVISTA galaxy survey fractal analysis in the *complete* sample. The single fractal dimensions D_L , D_z and D_G were obtained from this galaxy distribution respectively using the luminosity distance d_L , redshift distance d_z and galaxy area distance (transverse comoving distance) d_G .

	D_L	D_z	D_G
$z < 1$	1.44 ± 0.02	1.65 ± 0.02	1.80 ± 0.03
$1 \leq z \leq 6$	0.24 ± 0.01	0.30 ± 0.02	0.75 ± 0.06

traVISTA galaxy survey dataset comprising 220k objects spanning the redshift interval of $0.1 \leq z \leq 6$.

A reduced subsample of the survey was established by plotting the galaxies' absolute magnitudes in the J -band against their respective redshifts and setting an absolute magnitude cut with the apparent magnitude of $J = 24$, as well as a redshift cut at $z = 4$. Since this subsample showed that its galaxies followed increasing redshift bins, they were considered as effectively being a volume-limited distribution.

Fractal analysis of the reduced subsample was carried out using the standard Λ CDM relativistic cosmological model. As relativistic cosmologies have several definitions of observed distance, only three distinct ones were used here, namely the luminosity distance d_L , redshift distance d_z and galaxy area distance d_G , also known as transverse comoving distance. The use of several cosmological distance measures is due to the fact that relativistic effects become strong enough for redshift ranges larger than $z \gtrsim 0.3$, so these distance definitions produce different results for the same redshift value at those ranges. An algorithm for sorting the data according to the analytical developments required for testing an observed fractal structure as discussed here was also detailed.

The results indicate that the UltraVISTA subsample has two consecutive redshift ranges behaving as single fractal structures. For $z < 1$ the derived fractal dimension is well approximated by $D = (1.58 \pm 0.20)$, whereas for $1 \leq z \leq 4$ this dimension decreased to $D = (0.59 \pm 0.28)$. For comparison, the same fractal

analysis was also carried out in the complete survey data, yielding as well two consecutive redshift ranges characterized as single fractal systems: $D = (1.63 \pm 0.20)$ for $z < 1$ and $D = (0.52 \pm 0.29)$ in the range $1 \leq z \leq 6$. Both results, from the reduced and complete data, are consistent with those found by Conde-Saavedra et al. (2015), although here the conclusions were reached by a different, and simpler, methodology, and by applying this methodology to a numerically much larger galaxy sample in both cases.

The most obvious question regarding these results is why there is such a significant decrease in the fractal dimension for redshift values larger than the unity. Conceivably this might be due to an observational bias caused by the simple fact that many galaxies located beyond $z = 1$ are not being detected, decreasing then the observed galaxy clustering and, therefore, the associated fractal dimension at those scales. One might also consider the possibility of a bias in the galaxy number counts due to the small angular area of this survey. This means that its observational area might not provide a representative measurement of the entire sky distribution. Moreover it is important to consider the choice of observational field. If the size of the observed area is small and contains galaxy clusters, some galaxy concentration peaks can lead to higher fractal dimensions at low z .

It is also conceivable that the data used to obtain our results suffer from a detection bias related to the cumulative measure N_{obs} . Unbiasing this quantity might depend on comparing observed N_{obs} data with simulations derived from cosmological models' subsets and halo occupation distribution models (Berlind et al. 2003). One must also remember that the UltraVISTA photometric redshifts were obtained using SED fitting analysis, which means that the errors in the values are entirely dependent on the input assumptions used to derive these photo- z , and, therefore, it is not clear how the use of different types of photometric modeling might affect our results. This possible error source may be mitigated by the use of restricted galaxy samples, say, containing only luminous red galaxies such that photometric redshift uncertainties are minimized (Roza et al. 2016; Cawthon et al. 2018).

Another possible source of data uncertainty that might affect our results is the tension among the several measures of the Hubble constant. Here we have assumed the standard FLRW cosmological model with $H_0 = 70 \text{ km s}^{-1} \text{ Mpc}^{-1}$, nevertheless different Hubble constant predictions range this quantity by about $\pm 4 \text{ km s}^{-1} \text{ Mpc}^{-1}$. Relativistic cosmological models are known to be highly nonlinear, so how much this uncertainty in the Hubble constant might affect our results, if at all, cannot be quantified beforehand. So, to ascertain the possibly negligible, or otherwise, impact of this uncertainty in our results can only be concluded by actually carrying out the calculations with this parameter range and performing comparisons.

Aside from possible observational biases and yet unknown impact due to error sources, one might also attribute the decrease in the fractal dimension to a real physical effect. Perhaps, galaxy evolution dynamics is at play in causing such a decrease in the sense that there might be indeed much less galaxies at high z , meaning that the Universe was void dominated at those epochs since galaxies were much more sparsely distributed and in smaller numbers. Only further work with different high- z galaxy samples and in different regions of the sky may clarify this issue.

ACKNOWLEDGMENTS

We are grateful to the referee for useful comments. S.T. thanks the Universidade Federal do Rio de Janeiro for a PIBIC scholarship.

A.R.L. acknowledges Brazil's Federal Funding Agency CNPq for the financial support with a PCI fellowship.

REFERENCES

- Abdalla E., Chirenti C. B. M. H., 2004, *Physica A*, 337, 117
- Abdalla E., Afshordi N., Khodjasteh K., Mohayaee R., 1999, *A&A*, 345, 22
- Abdalla E., Mohayaee R., Ribeiro M. B., 2001, *Fractals*, 9, 451
- Albani V. V. L., Iribarrem A. S., Ribeiro M. B., Stoeger W. R., 2007, *ApJ*, 657, 760
- Amoroso Costa M., 1929, *Annals of Brazilian Acad. Sci.* (in Portuguese), 51, 1
- Berlind A. A., et al., 2003, *ApJ*, 593, 1
- Carpenter E. F., 1938, *ApJ*, 88, 344
- Cawthon R., et al., 2018, *MNRAS*, 481, 2427
- Charlier C. V. L., 1908, *Ark. Mat. Astr. Fys.*, 4, 1
- Charlier C. V. L., 1922, *Ark. Mat. Astr. Fys.*, 16, 1
- Coleman P. H., Pietronero L., 1992, *Phys. Rep.*, 213, 311
- Conde-Saavedra G., Iribarrem A., Ribeiro M. B., 2015, *Physica A*, 417, 332
- Cosmai L., Fanizza G., Sylos Labini F., Pietronero L., Tedesco L., 2019, *Class. Quantum Grav.*, 36, 045007
- De Vaucouleurs G., 1960, *ApJ*, 131, 585
- De Vaucouleurs G., 1970, *Science*, 167, 1203
- Einstein A., 1922, *Ann. Phys.*, 69, 436
- Ellis G. F. R., 1971, in Sachs R. K., ed., *General Relativity and Cosmology: Proceedings of the International School of Physics "Enrico Fermi", Course 47*. Academic Press, New York, pp 104–182. Reprinted in *Gen. Rel. Grav.*, 41 (2009) 581–660, doi:10.1007/s10714-009-0760-7
- Ellis G. F. R., 2007, *Gen. Rel. Grav.*, 39, 1047
- Etherington I. M. H., 1933, *Phil. Mag.*, 15, 761. Reprinted in *Gen. Rel. Grav.*, 39 (2007) 1055
- Gabrielli A., Sylos Labini F., Joyce M., Pietronero L., 2005, *Statistical Physics for Cosmic Structures*. Springer, Berlin
- Gaite J., 2007, *ApJ*, 658, 11
- Haggerty M. J., Wertz J. R., 1972, *MNRAS*, 155, 495
- Holanda R. F. L., Lima J. A. S., Ribeiro M. B., 2010, *ApJL*, 722, L233
- Holanda R. F. L., Lima J. A. S., Ribeiro M. B., 2011, *A&A*, 528, L14
- Holanda R. F. L., Lima J. A. S., Ribeiro M. B., 2012, *A&A*, 538, A131
- Hossienkhani H., Yousefi H., Azimi N., 2018, *Int. J. Geometric Methods Modern Phys.*, 15, 1850200
- Ilbert O., et al., 2013, *A&A*, 556, A55
- Iribarrem A. S., Lopes A. R., Ribeiro M. B., Stoeger W. R., 2012, *A&A*, 539, A112
- Jawad A., Butt S., Rani S., Asif K., 2019, *Eur. Phys. J. C*, 79, 926
- Jones B. J. T., Martínez V. J., Saar E., Einasto J., 1988, *ApJL*, 332, L1
- Mandelbrot B. B., 1983, *The Fractal Geometry of Nature*. Freeman, New York
- Martínez V. J., 1990, *Vistas in Astronomy*, 33, 337
- McCracken H. J., et al., 2012, *A&A*, 544, A156
- Mureika J. R., 2007, *J. Cosmology Astroparticle Phys.*, 2007, 021
- Mureika J. R., Dyer C. C., 2004, *Gen. Rel. Grav.*, 36, 151
- Nogueira F. A. M. G., 2013, Master's thesis, Valongo Observatory, Universidade Federal do Rio de Janeiro (arXiv:1312.5005)
- Pan J., Coles P., 2000, *MNRAS*, 318, L51
- Pietronero L., 1987, *Physica A*, 144, 257
- Raj V., Swapna M. S., Soumya S., Sankararaman S., 2019, *Indian J. Phys.*
- Rangel Lemos L. J., Ribeiro M. B., 2008, *A&A*, 488, 55
- Ribeiro M. B., 1992a, *ApJ*, 388, 1
- Ribeiro M. B., 1992b, *ApJ*, 395, 29
- Ribeiro M. B., 1993, *ApJ*, 415, 469
- Ribeiro M. B., 1994, in Hobill D. W., Burd A., Coley A., eds, B Vol. 332, *Deterministic Chaos in General Relativity*. Plenum, New York, p. 269 (arXiv:0910.4877), doi:10.1007/978-1-4757-9993-4_15
- Ribeiro M. B., 1995, *ApJ*, 441, 477
- Ribeiro M. B., 2001a, *Fractals*, 9, 237
- Ribeiro M. B., 2001b, *Gen. Rel. Grav.*, 33, 1699
- Ribeiro M. B., 2005, *A&A*, 429, 65
- Ribeiro M. B., Miguelote A. Y., 1998, *Brazilian J. Phys.*, 28, 132
- Rozo E., et al., 2016, *MNRAS*, 461, 1431
- Sadri E., Khurshudyan M., Chattopadhyay S., 2018, *Astrophys. Space Sci.*, 363, 230
- Scoville N., et al., 2007, *Astrophys. J. Supp. Series*, 172, 1
- Seley F., 1922, *Ann. Phys.*, 68, 281
- Souza B. J., 2020, Master's thesis, Physics Institute, Universidade Federal do Rio de Janeiro (in Portuguese)
- Stahl C., 2016, *Int. J. Modern Phys. D*, 25, 1650066
- Sylos Labini F., 2011, *Class. Quantum Grav.*, 28, 164003
- Sylos Labini F., Montuori M., Pietronero L., 1998, *Phys. Rep.*, 293, 61
- Wertz J. R., 1970, PhD thesis, University of Texas at Austin
- Wertz J. R., 1971, *ApJ*, 164, 227
- Zheng X., Liao K., Biesiada M., Cao S., Liu T.-H., Zhu Z.-H., 2020, *ApJ*, 892, 103

Paper prepared by the authors using L^AT_EX.